Remote Detection of Chemical Reactions using Nanoscale Terahertz Communication Powered by Pyroelectric Energy Harvesting

Eisa Zarepour, Mahbub Hassan, Chun Tung Chou
School of Computer Science and Engineering
University of New South Wales, Sydney, Australia
{ezarepour, mahbub, ctchou}@cse.unsw.edu.au

Adesoji A. Adesina*
ATODATECH LLC, Brentwood
CA 94513 USA
ceo@atodatech.com

ABSTRACT

A novel self-powered sensing and communication architecture for remote detection of chemical reactions is proposed. It is assumed that pyroelectric nanogenerators fitted with Graphene-based nano-antennas radiating in the Terahertz band (0.1-10THz) are embedded in the catalyst surface where different types of chemical reactions take place. Each reaction consumes or dissipates some heat, which causes temperature fluctuations on the catalyst surface. A pyroelectric nanogenerator harvests electrical energy from each temperature fluctuation and use the energy to transmit a THz pulse of proportional amplitude. Because different types of reactions dissipate different amounts of energy, we show that a remote receiver can detect the reaction type from the received pulse energy. The accuracy of reaction detection at the receiver, however, is compromised by the noise and attenuation of the THz channel, which makes it difficult to detect reactions from a longer distance. Using simulations, it is shown that dynamic frequency selection within the THz band based on the expected chemical composition of the reactor at any given time can help extending the distance of remote reaction detection.

1. INTRODUCTION

Live monitoring of reactions is important for measuring reactor conditions and improving the performance of chemical processes. Reaction monitoring is most commonly carried out via temperature and composition (and/or pressure) which still have to be used for inferential analysis of the catalyst conditions. However, if available, *direct information* on catalyst site properties and state offers significant opportunities for improving both catalyst and reactor technologies from a bottom-up perspective. Using wireless nanoscale sensor network to monitor and control chemical reactors has been recently demonstrated in the literature [8, 9, 11]. This paper proposes a novel self-powered wireless nanosensor network (WNSN) architecture for such direct monitoring of key reactions on the catalyst surface.

The proposed architecture exploits the observation that each reaction either dissipates (exothermic) or consumes (endothermic) certain amount of heat, which causes temporal variation in the ambient temperature. Therefore, a pyroelectric energy harvester [7] that harvests electrical energy from the temporal gradient in ambient temperature, can be readily used to power a nanosensor node deployed in a catalyst site. Furthermore, because the exact amount of dissipated or consumed heat strongly depends on the type of reactions, the reaction type can be inferred from the harvested pyroelectric energy. Thus, the pyroelectric energy harvester could play the dual role of an *energy generator* as well as a *reaction sensor*. The remaining challenge is to wirelessly transfer the information from nanoscale devices to macroscale sinks, so the reactions can be monitored from the Internet.

To enable wireless monitoring, we propose that the pyroelectric nanogenerators are fitted with Graphene-based nano-antennas [5] capable of radiating in the Terahertz band (0.1-10THz). When a reaction takes place, the nanogenerator use the harvested energy to transmit a THz pulse of proportional amplitude. Because different types of reactions dissipate different amounts of energy, a remote receiver should be able to detect the reaction type from the received pulse energy.

The performance of the proposed WNSN-based remote reaction monitoring architecture is evaluated using a specific chemical reactor called Fischer-Tropsch Synthesis (FTS), which converts gas to liquid. We find that the molecular absorption (attenuation) and noise of the THz channel are major barriers for accurate reaction detection at the sink. Detection accuracies over 90% cannot be achieved beyond 0.5 mm, which makes it challenging to connect the WNSN to the Internet.

Because molecular absorption and noise are highly frequency selective, we propose to divide the THz band into many subchannels and select a subchannel that is least affected by the molecular composition of the reactor environment as a means to overcome the THz challenge. Simulation experiments show that by dynamically selecting the subchannels during the chemical process, accurate reaction detection ($> 90\%$) can be achieved at a distance of 50 cm

*This work was initiated while the author was with the School of Chemical Engineering at University of New South Wales, Sydney, Australia.

DOI: http://dx.doi.org/10.1145/2800795.2800820 .

from the nanogenerator, which makes Internet-based remote reaction monitoring feasible. The key contributions of this paper can be summarised as follows:

- We propose a novel self-powered WNSN architecture for reaction monitoring that uses *reaction heat* as a source of energy harvesting as well as reaction detection
- We build a performance model to study the reaction detection accuracies of the proposed architecture
- We simulate a widely used commercial reactor and show that the default use of the entire THz band as a *single channel* cannot achieve accurate reaction detection beyond 0.5 mm
- We show that *dynamic frequency selection* within the THz band can help achieve accurate reaction detection at significantly longer distances making it feasible to connect the WNSN to the Internet.

The rest of this paper is structured as follows. Details of the proposed WNSN architecture are discussed in Section 2. Performance modelling of remote reaction detection over THz channel is presented in Section 3, followed by the simulation results in Section 4. We conclude the paper in Section 5.

2. REACTION MONITORING ARCHITECTURE

The proposed WNSN-based reaction monitoring architecture is shown in Figure 1. A chemical reactor contains one or many tubes designed to allow the processing of chemical reactants via different reactions under specified pressure and temperature in the presence of a catalyst (figure 1.a). The inner surface of a catalyst tube contains numerous *sites* (figure 1.c) where reactants adsorb and react with each other producing different chemicals. It is assumed that each catalyst site is fitted with a pyroelectric nanogenerator coupled with a Graphene antenna for wireless transmission in the THz band (figure 1.d). We also assume that we can deploy a rod through the axis of the catalyst tube to embed few macroscale wireless remote sink connected to the Internet (figure 1.b). The communication medium between nanomotes and the remote sinks therefore consists of the chemicals inside the tube. The types and amounts of these chemicals change as the chemical production proceeds. The remote sinks are connected to the Internet through a wireless gateway located outside of the reactor.

In order to make our discussion concrete, we have selected FTS [1] as a case study. However, the discussion and methodology in this paper is entirely general. FTS synthesis is a major process for converting natural gas to liquid hydrocarbons in a chemical reactor. The reactor starts with a specific amount of carbon monoxide (CO) and hydrogen (H_2). Many chemical species are produced and consumed via 8 different categories (types) of reactions, R_1 to R_8 which have been presented in Table 1 along with the amount of generated heats. We assume an iron-based fixed-bed FTS reactor which has catalyst sites with dimensions of $0.3\mu m \times 0.3\mu m$, so the mass of each site is around 1.5fg. We propose that a rod be deployed inside through the axis of the catalyst tube at a given distance containing macro-scale wireless remote sinks connected to the Internet.

Table 1: Elementary Reactions and Released Energy in KJ/mol for Fischer-Tropsch Synthesis

	Reaction	**Released Energy (KJ/mole)**
Adsorption Phase		
1	$CO \longrightarrow C_{(s)} + O_{(s)}$	56.81±0.96
2	$H_2 \longrightarrow H_{(s)} + H_{(s)}$	10±0.5
Water Formation		
R_1	$O_{(s)} + H_{(s)} \longrightarrow OH_{(s)} + s$	103.80±0.96
R_2	$OH_{(s)} + H_{(s)} \longrightarrow H_2O_{(s)} + s$	86.22±0.62
Chain Initiation		
R_3	$C_{(s)} + H_{(s)} \longrightarrow CH_{(s)} + s$	77.66 ±0.7
R_4	$CH_{(s)} + H_{(s)} \longrightarrow CH_{2(s)} + s$	11.94±0.1
R_5	$CH_{2(s)} + H_{(s)} \longrightarrow CH_{3(s)} + s$	61.88±0.5
Chain Growth		
R_6	$C_nH_{2n+1(s)} + CH_{2(s)} \longrightarrow C_mH_{2m+1(s)}$ (m=n+1)	44.79±0.43
Hydrogenation to Paraffin (HTP)		
R_7	$C_nH_{2n+1(s)} + H_{(s)} \longrightarrow C_nH_{2n+2} + 2s$	117.75±0.67
β -Dehydrogenation to Olefin (DTO)		
R_8	$C_nH_{2n+1(s)} \longrightarrow C_nH_{2n} + H_{(s)}$	96.27±0.5

The pyroelectric nanogenerator converts any temperature variation to electricity. The generated pyroelectric current I is proportional to the *rate of temperature change* and is obtained as $I = P_C \times A \times (\frac{dT}{dt})$, where P_C is the *pyroelectric current coefficient* of the material (80 $\mu nC/cm^2K$ [7]), A is the electrode area ($0.3\mu m \times 0.3\mu m$), and dT/dt is the rate of change in temperature. The harvested power is then derived as $P_H = I^2 \times R$, where R is the device resistance (50 MΩ in [7]).

To compute the pyroelectric power, we need to derive the rate of temperature change, which can be obtained as $\frac{dT}{dt} = \frac{\Delta T}{t}$, where ΔT is the amount of temperature rise in the site due to the reaction heat and t is the reaction time. ΔT can be obtained directly from the heat formula as $\Delta T = \frac{H}{C_p \times m}$, where H is the amount of reaction heat released to the site, C_p is the heat capacity (*specific heat*) of the catalyst material (0.45 J/gK for iron), and m is the mass of the reaction *site* (1.5fg). Assuming that it takes 1 ps for a reaction to complete, we have $\frac{dT}{dt} = \Delta T \times 10^{12}$. This means that even for a small ΔT, we can expect a significant rate of change in the temperature and eventually the harvested power. Figure 2 shows the temperature rise in each site of an iron-based catalyst and the resulting harvested power using the pyroelectric model of [7]. The figure suggests that each nanomote can harvest averagely 10nW per reaction.

Now let us explain the working principle. When a reaction occurs in a catalyst site, production (or consumption) of heat by the reaction would increase (or decrease) the temperature of the site. This instantaneous temperature variation will be converted to electrical energy by the Pyro-EH. The nanoradio use this harvested power to directly generate and transmit a radio pulse to a nearby remote sink. Because the power amplitude of the pulse is proportional to the harvested energy, it should be possible to use the received energy of the pulse at the remote station to differentiate one type of reaction from another. Although different types of reactions

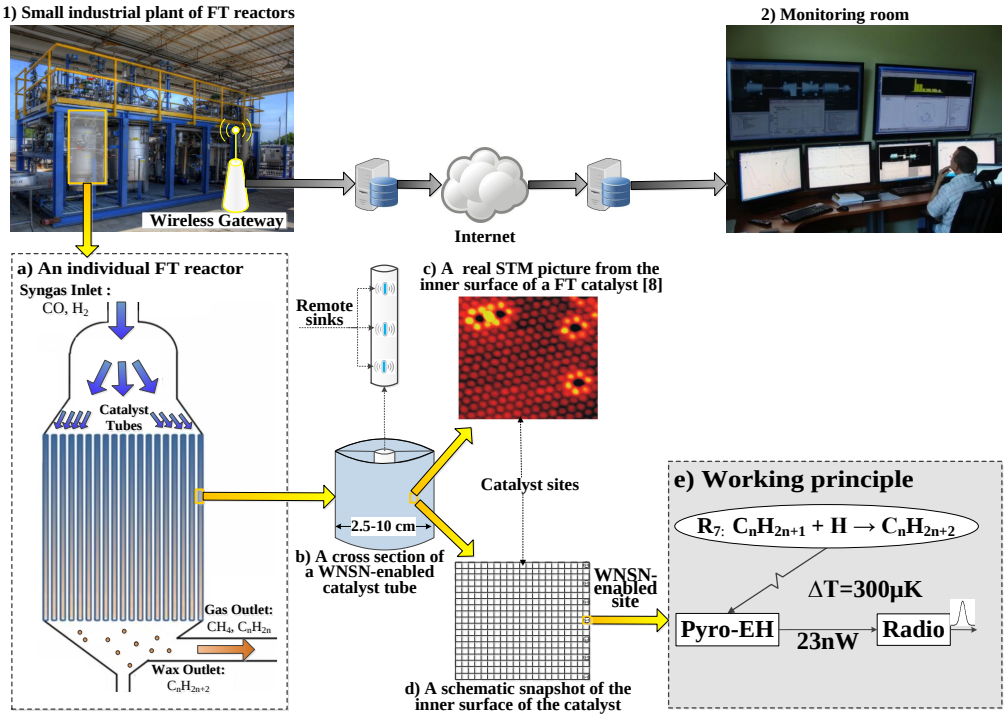

Figure 1: Overall microscopic monitoring of chemical reactor using WNSN. (1) a picture from a small industrial plant of FT reactors. (2) data from the reactor will be collected and transferred to the monitor room for further analysis. (a) schematic of a single chemical reactor. (b) a snapshot from of a cross section of a catalyst tube. (c) a STM picture from the inner surface of a real FT catalyst tube [6] (d) a schematic of the inner surface of the catalyst that its sites have been equipped with the proposed nanomotes. (e) the working principle of the proposed architecture in reaction monitoring. As an example, an R_7 reaction raises the site temperature by $300\mu K$, which generates a 23 nW of instantaneous power supply for the radio.

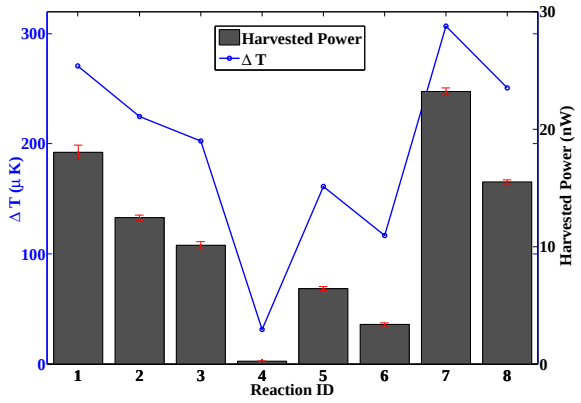

Figure 2: Estimating harvested power from temperature rise in a site.

produce different amounts of energies, the actual received pulse energies at the sink would depend on the amount of noise and signal attenuation experienced by the transmitted pulses in the THz channel, making accurate wireless reaction detection a challenging problem. In the next section, we propose a performance model to capture the reaction detection accuracy using the proposed architecture.

3. PERFORMANCE MODEL

Due to molecular absorption and noise of the THz band, the received pulse energy at sink becomes a random variable. The received pulse energy of different reactions then could overlap with each other, making accurate reaction detection a challenging problem. In this section, we propose a performance model to evaluate the accuracy of wireless reaction monitoring at a given distance using the proposed architecture. First, we describe the reaction model followed by characterizing the THz channel within a chemical reactor, and finally the accuracy model of reaction detection using a threshold based decoder at the sink.

3.1 Reaction model

Our aim is to use the proposed architecture to monitor a set of M possible chemical reactions $r_1, r_2, \ldots, r_M$. We assume that when the reaction of type r_i occurs, it emits $E_{e,i}$ amount of energy and all $E_{e,i}$'s are distinct. For a reason which will become clear in Section 3.4, we assume that the reaction types are ordered in ascending order of reaction emission energy, i.e. $E_{e,1} < E_{e,2} < ... < E_{e,M}$.

The emitted energy via each reaction is used to generate and transmit a Gaussian pulse using a nanoscale Graphene based nanoantenna which operate over THz band. A key problem in using the terahertz band within a chemical reactor for communication is that the variation in the composition of the reactor, due to occurrence of different reactions,

creates a time-varying communication channel [10]. In the next section, we overview the time varying terahertz channel modelling.

3.2 THz channel model

We consider a single-hop communication via a radio channel in a wireless medium which has time-varying chemical composition. Radio communication is affected by the chemical compositions, i.e., existing molecules in the channel, in two different ways in the terahertz band. First, radio signal is attenuated because molecules in the channel absorb energy in certain frequency bands. Second, this absorbed energy is re-radiated by the molecules to create noise in the channel.

We assume the radio channel is a medium consisting of N chemical species $S_1, S_2, ..., S_N$. The effect of each chemical species S_i on the radio signal is characterised by its molecular absorption coefficient $K_i(f)$ of species S_i at frequency f. The molecular absorption coefficients of many chemical species are available from the HITRAN database [2]. Let $m_i(t)$ be the mole fraction of chemical species S_i in the medium at time t. The medium absorption coefficient $K(t, f)$ at time t and frequency f is a weighted sum of the molecular absorption coefficients in the medium:

$$K(t, f) = \sum_{i=1}^{N} m_i(t) K_i(f) \tag{1}$$

The medium absorption coefficients $K(t, f)$ determines the attenuation and the molecular absorption noise in the radio channel. Let d denote the distance between the nanomote and the remote station. The total attenuation due to spreading and molecular absorption at time t, frequency f and a distance d from the radio source, $A(t, f, d)$, is given by [4, 10]:

$$A(t, f, d) = \left(\frac{4\pi f d}{c}\right)^2 e^{K(t,f)d} \tag{2}$$

where c is the speed of light.

The PSD of the received signal $P_{r,i}(t, f, d)$ at frequency f, time t and distance d is:

$$P_{r,i}(t, f, d) = \frac{U_i(f)}{A(t, f, d)} \tag{3}$$

The average received energy for a given reaction of r_i at time t then would be:

$$E_{r,i}(t, d) = \int_B P_{r,i}(t, f, d) T_p df \tag{4}$$

where T_p is the duration of the transmitted pulse in second. The PSD of the molecular absorption noise $N_{\text{abs}}(t, f, d)$ which is due to the re-radiation of absorbed radiation by the molecules in the channel is given by [4]:

$$N_{\text{abs}}(t, f, d) = k_B T_0 (1 - \exp(-K(t, f) * d)) \tag{5}$$

where T_0 is the reference temperature 296K and k_B is the Boltzmann constant. Amusing a flat noise spectrum, the noise PSD at distance d would be:

$$N(t, d) = \frac{\int_B N_{\text{abs}}(t, f, d) df}{B} \tag{6}$$

3.3 Receiver model

The receiver model aims to characterised the signal received by the remote station. We assume that a reaction of type r_i, where $i = 1, .., M$ has occurred at the nanomote. The reaction of type r_i generates an energy of $E_{e,i}$. We assume both the energy harvester and the nanoradio are ideal, which means the nanomote generates a pulse with energy $E_{e,i}$ to be transmitted to the remote station. (Note that inefficiency in energy harvesting and radio can be taken care of easily.) We further assume that the pulse generated by the nanoradio has a duration of $T_p = 10^{-13}s$ and its power spectral density (PSD) uniformly spread in the 0.1-10 THz band. We denote $B = 10$ THz as the bandwidth of the pulse and $U_i(f)$ as the PSD of the transmitted signal at frequency f when reaction type e_i occurs.

The remote station uses an energy detector (ED) to determine the energy level of the received signal. The ED requires the design of a filter, matched to the received pulse shape. We assume the bandwidth of the filter is equal to B. If an reaction of type r_i occurs at the nanomote, the received energy level has a Gaussian distribution of g_i with mean μ_i and variance σ_i^2 given by [3]:

$$\mu_i = N T_{\text{int}} B + E_{r,i} \tag{7}$$

$$\sigma_i^2 = N^2 T_{\text{int}} B + 2N \times E_{r,i} \tag{8}$$

where N is the noise PSD at distance d that can be calculated from equation 6, $E_{r,i}$ is the average received energy for symbol r_i that can be calculated from equation 4. T_{int} is the integration time which is a design parameter, typically $T_{int} >= T_p$.

3.4 Accuracy of reaction detection

This section presents the threshold-based decoder (TBD) which uses the received energy at the remote station to determine the reaction that has occurred at the nanomote. Recall from Section 3.3 that if reaction type r_i has occurred, then the received energy has a Gaussian distribution with mean μ_i and variance σ_i^2 given in Eq. (7) and (8). Also, recall from Section 3.1 that for two reaction types r_i and r_j with $i < j$, we have $E_{e,i} < E_{e,j}$ where $E_{e,i}$ and $E_{e,j}$ are respectively the energy emitted when the reaction types r_i and r_j occurs. Consequently, we have $\mu_i < \mu_j$ for $i < j$ or the mean received energies μ_i are sorted in ascending order.

In order to distinguish between the M reaction types, we need $M - 1$ different thresholds, which are denoted by $\xi_{1,2}$, $\xi_{2,3}$, ..., and $\xi_{M-1,M}$. The value of $\xi_{i,j}$ ($i = 1, ..., M - 1$ and $j = i + 1$) is given by the intersection of the Gaussian density functions with parameters (μ_i, σ_i^2) and (μ_j, σ_j^2), i.e. $\xi_{i,j}$ satisfies

$$f_{N_i}(\xi_{i,j}) = f_{N_j}(\xi_{i,j}) \tag{9}$$

$$\frac{1}{\sqrt{2\pi}\sigma_i} e^{\frac{-(\xi_{i,j}-\mu_i)^2}{(2\sigma_i^2)}} = \frac{1}{\sqrt{2\pi}\sigma_j} e^{\frac{-(\mu_j-\xi_{i,j})^2}{(2\sigma_j^2)}} \tag{10}$$

and we have $\mu_i < \xi_{i,j} < \mu_j$.

Let e_r be the received energy at the remote station, then the estimated reaction type $\hat{i}$ is determined according to:

$$\hat{i} = \begin{cases} 1 & \text{if } e_r < \xi_{1,2} \\ i & \text{if } \exists i \in \{2, 3, ..., M-1\} \; s.t. \; \xi_{i-1,i} < e_r < \xi_{i,i+1} \\ M & \text{if } e_r > \xi_{M-1,M} \end{cases} \tag{11}$$

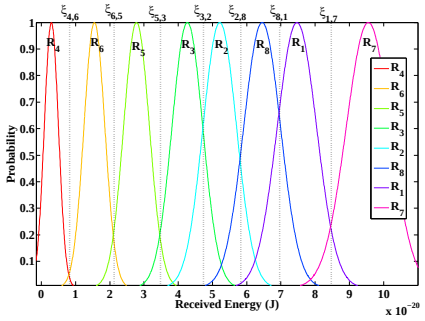

(a) d=0.6mm, error=0.14, Noise=1×10^{-21}

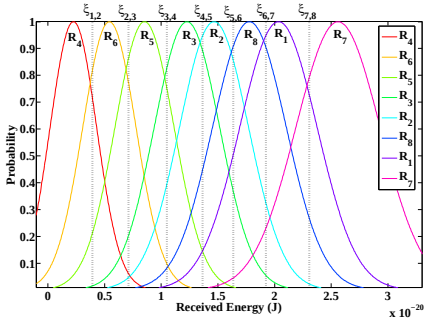

(b) d=6mm, error=0.43 , Noise=2×10^{-21}

Figure 3: The impact of distance on the accuracy of event detection. Received pulse energies for each reaction at the receiver in two different distances.

It can be shown that the error probability $P_{e,TBD}$ of the TBD method is given by:

$$P_{e,TBD} = P[E_r > \xi_{1,2}|r_1]P[r_1] + \sum_{i=2}^{M-1}(P[E_r < \xi_{i-1,1}|r_i] + P[E_r > \xi_{i,i+1}|r_i])P[r_i] + P[E_r < \xi_{M-1,M}|r_M]P[r_M] \quad (12)$$

where $P[r_i]$ is the probability that reaction type r_i occurs, E_r is the random variable of received energy at the remote station and $P[E_r > \xi|r_i]$ is the conditional probability that the received energy is greater than ξ given that the reaction type r_i has occurred. Note that the conditional probability is in fact a Gaussian distribution with mean μ_i and variance σ_i^2. Therefore, given the reaction model and the receiver model, it is possible to determine the classification error.

Assuming an equal probability for all 8 types of FT reactions, Figure 3 shows the received signal energies at the remote station along with 7 thresholds which has been calculated for two distances (0.6mm and 6mm) in a given FT composition (CO:35%, H:62%, OH+H_2O =0.5%, others < 2.5%). In the first case, as the noise lower, due to smaller distance, the received signal energies have less overlap which leads to lower error (14%) than the second case (43%). However, for a given distance, as the composition during the FT reactor is variable, the calculated thresholds would be dynamic over time. In the next section, we simulate a real FT reactor to analyse possible reaction accuracy over different distances.

4. RESULTS

In this section, we simulate a real FTS reactor and investigate the performance of the proposed reaction monitoring architecture.

4.1 Methodology

We assume the FT process starts with 100 carbon monoxide molecules and 250 hydrogen atoms. We assume a conventional fixed-bed iron FT catalyst with equal kinetic constants of 10 for all possible reactions except water formation reactions that has been considered as 0.07 and 2 for $O + H \longrightarrow OH$ and $OH + H \longrightarrow H_2O$, respectively. The chemical production continues until no more new chemicals can be produced. Molecular absorption coefficient of the chemical species produced within the reactor is obtained from the HITRAN database [2] for a temperature of 500K and pressure of 10 atmospheres. for a given channel composition, we follow the procedure in Section 2 to compute the medium absorption coefficient, attenuation, molecular noise and received signal energies at the remote station in a given distance. Then, we use the performance model of section 3 to calculate the thresholds and finally the error of the reaction detection. As the composition of the medium is variable over time, we have different levels of error at different time slots, so we present the average error during the FTS in all experiments.

We simulate three different methods of using the THz band. In the first, which we call *Default THz*, the entire band (0.1-10THz) is used as a single channel having a 9900 GHz bandwidth. In the second and third, the THz is divided into N subchannels of equal (9900/N GHz) bandwidth, but only one of these N channels are used at any given time. In the second method, nanogenerators select the subchannel that has the minimum absorption coefficient during the entire synthesis. We refer to this method as *static channel selection* (SCS), as the subchannel is selected once in the beginning and used throughout the chemical process without any channel change. In the third method, we obtain the evolution of the FTS composition over time via extensive offline simulations and then derive the subchannels with the lowest absorption at any time slot. Then, the nanogenerators use this information as a vector of (time, frequency) to dynamically switch to the appropriate subchannel at any time slot. We refer to this method as *dynamic channel selection* (DCS). More details on SCS and DCS are available in [10].

4.2 Simulation Results

Figure 4 plots the average probability of error for reaction detection at the sink for 20 different distances ranging from $0.1\mu m$ to $0.1m$ when the entire THz band is used in the default mode as a single channel. It shows that the error is almost zero for distances less than 0.5mm, but starts to increase exponentially after that. This exponential increase is due to the exponential rise in the molecular noise and attenuation of the THz channel (see Equations. 2 and 5). We define *effective monitoring distance*, η, as the distance at which reactions can be detected in the remote sink with less than 10 % error. As it can be seen from Figure 4, to achieve reaction detection accuracy over 90%, the sink cannot be further than $0.5mm$ ($\eta = 0.5mm$) from the pyroelectric nanogenerators. However, it is difficult to install large macroscale receivers with Internet connectivity so close

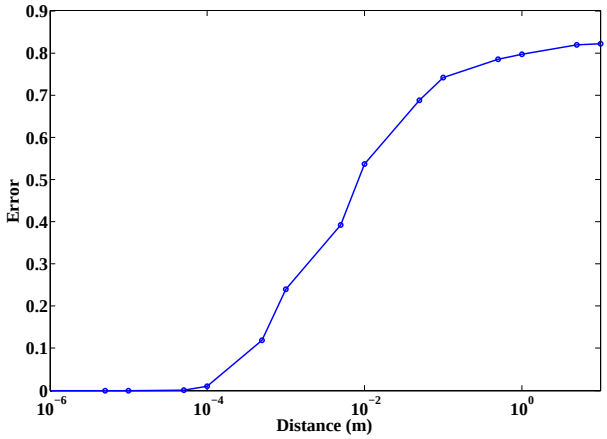

Figure 4: Reaction detection accuracy for Default THz as a function of distance between nanogenerator and sink.

to the catalyst. Next, we investigate the improvements that

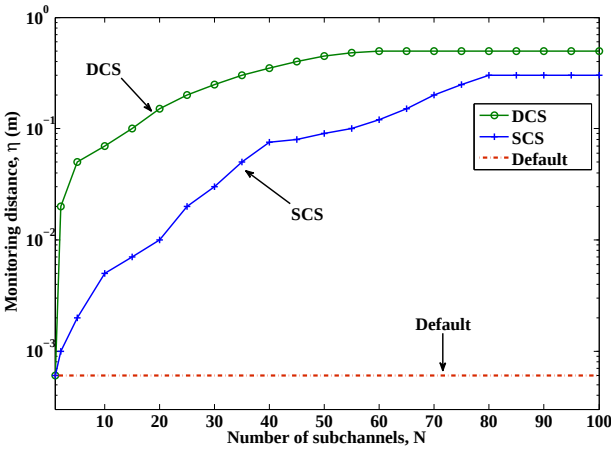

Figure 5: Effective wireless reaction monitoring distance (η) as a function of number of THz sub-channels.

can be achieved with multi-channel THz. Figure 5 shows the effective monitoring distance (η) as a function of number of subchannels N. For both SCS and DCS, effective monitoring distance initially increases with increasing number of subchannels, but stops increasing after a threshold. While η is less than 0.5mm for the Default THz, it extends to 25 cm with SCS when the THz band is divided into 80 subchannels with 123.75 GHz channel bandwidth. Finally, with DCS we can achieve wireless reaction monitoring from a distance of 50 cm by using 60 subchannels each having 166.6GHz bandwidth. These extensions make it much easier to connect the WNSN to the Internet.

5. CONCLUSIONS

Using simulations, we have shown that *reaction heat* can be used both as a source of energy harvesting for nanosensor nodes as well as reaction detection. In principle, remote reaction detection is possible by using the harvested energy to transmit a THz pulse of proportional amplitude, because different reactions generate different amounts of energy. In reality, the molecular absorption and noise of the THz band make it difficult to achieve accurate reaction detection beyond a few hundred micrometers. We have, however, found that *dynamic frequency selection* within the THz band enables accurate reaction detection at significantly longer distances making it feasible to monitor reactions from the Internet.

6. REFERENCES

[1] A. Adesina. Hydrocarbon synthesis via Fischer-Tropsch reaction: travails and triumphs. *Applied Catalysis A: General*, 138(2):345–367, 1996.

[2] Y. L. Babikov, I. E. Gordon, and S. N. Mikhailenko. Hitran on the web, a new tool for hitran spectroscopic data manipulation. In *the Proceeding of the ASA-HITRAN Conference*, Reims, France, Aug 29-31, 2012.

[3] S. Cui and F. Xiong. M-ary energy detection of a Gaussian FSK UWB system. *EURASIP Journal on Wireless Communications and Networking*, 2014(1):87, 2014.

[4] J. Jornet and I. Akyildiz. Channel modeling and capacity analysis for electromagnetic wireless nanonetworks in the terahertz band. *IEEE Transactions on Wireless Communications*, 10(10):3211–3221, 2011.

[5] J. M. Jornet and I. F. Akyildiz. Graphene-based Plasmonic Nano-transceiver for Terahertz Band Communication. In *8th European Conference on Antennas and Propagation (EuCAP)*, pages 2–6, The Hague, The Netherlands, 2014.

[6] P. C. Thüne, C. J. Weststrate, P. Moodley, a. M. Saib, J. van de Loosdrecht, J. T. Miller, and J. W. Niemantsverdriet. Studying Fischer Tropsch catalysts using transmission electron microscopy and model systems of nanoparticles on planar supports. *Catalysis Science & Technology*, 1(5):689, 2011.

[7] Y. Yang, S. Wang, Y. Zhang, and Z. L. Wang. Pyroelectric nanogenerators for driving wireless sensors. *Nano letters*, 12(12):6408–13, Dec. 2012.

[8] E. Zarepour, A. A. Adesina, M. Hassan, and C. T. Chou. Nano Sensor Networks for Tailored Operation of Highly Efficient Gas-To-Liquid Fuels Catalysts. In *Australasian Chemical Engineering Conference*, Brisbane, Australia, 29 Sep - 2 Oct, 2013.

[9] E. Zarepour, A. A. Adesina, M. Hassan, and C. T. Chou. Innovative approach to improving gas-to-liquid fuel catalysis via nanosensor network modulation. *Industrial and Engineering Chemistry Research*, 53(14):5728–5736, 2014.

[10] E. Zarepour, M. Hassan, C. T. Chou, and A. Adesina. Frequency Hopping Strategies for Improving Terahertz Sensor Network Performance over Composition Varying Channels. In *The IEEE WoWMoM 2014*, Sydney, Australia, June, 2014.

[11] E. Zarepour, M. Hassan, C. T. Chou, and A. A. Adesina. Nano-scale Sensor Networks for Chemical Catalysis. In *the Proceedings of the 13th IEEE International Conference on Nanotechnology*, Beijing, China, 2013.